I J C T A, 6(1) June 2013, pp. 1-14

Performance of Lifting-circular Wavelet Scheme for Signal Acquisition in GNSS Receivers

[1]Chung-Liang Chang[*], [2]Ho-Nien Shou and [3]Jyh-Ching Juang

ABSTRACT

This study proposes a novel method to acquire the navigation signal parameters for Global Navigation Satellite System (GNSS). This method utilizes modified discrete wavelet transformer (MDWT) to reduce operation samples of circular convolution during signal acquisition process and to divide the wavelet space, indicating that the MDWT is better in de-correlation ability and signal acquisition performance. Besides, it can cut down the effect of noise and interference on signal acquisition performance and enhance the signal to noise ratio on the basis of priori knowledge of the signal characteristics. Simulations and experiments demonstrate that the proposed method can improve performance in shorten acquisition time and lower computation complexity as opposed to traditional fast Fourier transform (FFT) based methods.

Keywords: FFT; discrete wavelet transform; synchronization, spread spectrum code, GNSS

I. INTRODUCTION

GPS has been widely applied to military and civilian aspects and this system transmits different positioning information through each satellite so that users can obtain the information of latitude, longitude, time, and speed. Each satellite transmits positioning signal in L1/L2 band. The receiver available in market consists of single or dual-band received mode and the more prevalent one is the cheaper single-band receiver, which only receives modulated signal in L1 band, when the satellite transmits L1 signal, a receiver can produce a synchronized copy of the code and multiply it by the received signal. If the local code is suitable synchronized, its correlation with the original signal is maximum; otherwise the correlation is rather low.

The signal synchronization process is called signal acquisition, which consists of signal search and signal detection. The major goal is to find initial code offset and Doppler shift so as to calculate pseudo range. Meanwhile, satellite ephemeris data is adopted to calculate user location. Thus, the accuracy of pseudo range does affect the positioning precision of GPS receiver. The major error source that affects signal acquisition performance and leads to range error is thermal noise. Typically speaking, the noise can result in positioning error of 0-10 meters [1][2]. With the intentional and unintentional interference, the GPS receiver can't function properly. The most common signal acquisition methods, such as time-domain search method, frequency-domain search method [3], etc, adopt longer non-coherent integration time for thermal noise to successfully acquire signal, which inevitably increases the computation time. Fast acquisition methods usually use circular convolution to perform the correlation of all code delays at once, for each Doppler bin. Circular convolution is achieved through frequency domain multiplication because the incoming

1 Department of Biomechatronics Engineering, National Pingtung University of Science and Technology, Pingtung County, Taiwan, *E-mail: *chungliang@mail.npust.edu.tw* (corresponding author)

2 Department of Avionics Communication & Electronics, Air Force Institute of Technology, Kaohsiung County, Taiwan, *E-mail: longlifeshow@xuite.net*

3 Department of Electrical Engineering, National Cheng Kung University, Tainan City, Taiwan, *E-mail: juang@mail.ncku.edu.tw*

and local code sequences are of finite duration. Nevertheless, the hardware complexity is increased due to the number of fast Fourier transform (FFT) blocks and the length of that block. Decimated/interpolation methods can be utilized for improvement. Interpolation and decimation are operations utilized to magnify and reduce sampled signals, respectively, through an integer factor. Regarding magnification of a sampled signal, the new value values, not present in the signal, should be computed and inserted among the existing samples. Estimation of the new value is calculated from a neighborhood of the samples of the original signal. Likewise, a new value in decimation is estimated from a neighborhood of samples and replaces these values in the minimized signal. Implementation of integer factor interpolation and decimation algorithms can be conducted through efficient finite impulse response (FIR) filter and are relatively fast. Note that it can be efficient to process data at a different sampling frequency than one given in a data set. The reason for utilizing decimation of the GPS signal is not only to reduce the size of the data set but also optimize the data set size for FFT algorithm. One published paper employ this method to solve this problem and it is implemented on digital signal processing (DSP) test board [4].

In resent years, a frequency-time analysis method has been utilized in signal decomposition, which is called wavelet transform. In early stage, this technique is simply used in mathematical domain. Later, it is applied to digital signal processing through the research of Daubechies [5], Mallat [6]. In its discrete form, signals are decomposed by so called compact supported base functions, which may be time- and frequency limited. Contrary to the Fourier transformation, this leads to a high precision in time and frequency resolution. Currently, this method is often used in GNSS signal acquisition [7] [8]. However, its computation load is too large due to its limitation in original design. Thus, Sweldens proposed a simplified Wavelet structure, whose converted coefficient of wavelet is the same as that of conventional wavelet filter. It hardware resource is only half of the original structure [9].

Consequently, this paper proposes a signal acquisition strategy, which changes the traditional signal acquisition process [3] and utilizes modified wavelet transformer to reduce operation samples of circular convolution during signal acquisition process. Besides, it can cut down the effect of noise and interference on signal acquisition performance and enhance the signal to noise ratio on the basis of priori knowledge of the signal characteristics. This method is not only effective in reducing the complexity of hardware implementation, but is also robust in signal acquisition performance.

II. METHODOLOGY

(A) Signal model

The signal processing of internal baseband in GPS receiver consists of signal search, detection, tracking and de-navigation message. The paper focuses on signal search and detection. Thus, the whole signal mathematical expression will be elaborated.

Assume the satellite signal is received through the front-end of receiver and is processed through down-converted operation and analog-to-digital converter, the digital baseband signal is expressed as follows:

$$y[k] = \sum_{n=0}^{N} \sqrt{2P_n}\, x_n(kT_s - \tau_n) \exp\{2\pi(f_B + f_D)kT_s + \phi_n\} + w[k] \tag{1}$$

where L denotes the number of visible satellites in sky, P_n represents the power of n-th satellite signal, w is noise, k indicates index of discrete signal sequence, $T_s = 1/f_s$ stands for sampling rate, f_B and f_D denote frequency of baseband and Doppler shift, respectively. $x_n(kT_s) = x_n[k]$ represents the n-th satellite baseband sequence, which is composed of sub-carrier, pseudo random code and navigation message. In the GPS C/A signal, sub-carrier is the periodic repetition of a rectangular pulse and $x_n[k]$ is binary phase shift key (BPSK) modulated with a chipping rate equal to 1.023 MHz. The goal of signal search is to find the initial

synchronization point of coarse code sequence and Doppler frequency to conduct subsequent signal detection and tracking signal detection and tracking. Thus, how to accurately and rapidly find τ_n and f_D and efficiently reduce the internal hardware complexity of receiver is the major concern of this research. The following will depict the result and design of proposed method.

(B) Proposed Scheme

The proposed signal acquisition structure is based on the modified discrete wavelet transform proposed by Sweldens [9] and applies it to GPS signal acquisition. The modified wavelet structure and conventional wavelet transform are the same, which consist of analysis filter bank and synthesis filter bank. The major difference lies in the design structure of bank. In terms of modified wavelet transform structure, the analysis filter bank is divided into splitting module, lifting module, scaling module. In splitting module, the input signal is divided into odd discrete signal $y_0^L[2k+1]$ and even discrete signal $y_0^L[2k]$. After the signal is 1/2 sampled, $\overline{y}_0^H[k]$ and $\overline{y}_0^L[k]$ are obtained. In lifting module, $\overline{y}_0^L[k]$ passes through a predict operation unit *P*, which can yield a predicted value. The error between the predicted value and desired signal $\overline{y}_0^H[k]$ denotes a high frequency wavelet coefficient $\overline{c}_1^H[k]$, which is given by:

$$\overline{c}_1^H[k] = \overline{y}_0^H[k] - P(\overline{y}_0^L[k]) \tag{2}$$

Then, $\overline{c}_1^H[k]$ passes through a compensate operation unit *U*, which can yield a predicted value. The addition of predicted value and $\overline{y}_0^L[k]$ produces a low frequency wavelet coefficient $\overline{s}_1^L[k]$, which is written as:

$$\overline{s}_1^L[k] = \overline{y}_0^L[k] + U(\overline{c}_1^H[k]) \tag{3}$$

In scaling module, low-frequency wavelet coefficient $\overline{s}_1^L[k]$ and high-frequency $\overline{c}_1^H[k]$ multiply constant g_L and g_H, respectively. That is to normalize the two coefficients, which is expressed as:

$$c_1^H[k] = g_H \overline{c}_1^H[k] \tag{4}$$

$$s_1^L[k] = g_L \overline{s}_1^L[k] \tag{5}$$

Another aspect is synthesis of modified wavelet transform, which is also called inverse wavelet transform. This structure consists of three parts, such as scaling module, lifting module and merging module. The structure is similar to modified discrete wavelet decomposition and their complexity is the same, which is given by:

$$\hat{\overline{y}}_0^H[k] = \hat{\overline{c}}_1^H[k] + P(\hat{\overline{y}}_0^L[k]) \tag{6}$$

$$\hat{\overline{y}}_0^L[k] = \hat{\overline{s}}_1^L[k] - U(\hat{\overline{c}}_1^H[k]) \tag{7}$$

The converted wavelet coefficient of modified wavelet structure is the same as that of traditional wavelet filter. The former is low in implementation complexity. In particular, the wavelet coefficient of filter can be implemented using the integer addition and shift register, which results in shorter computation time.

The wavelet transform in analysis filter bank process operates in terms of first-level, second-level, etc. In first-level, the input signal is decomposed into high frequency component $c_1^H[k]$ and low frequency component $s_1^L[k]$. The low frequency component is provided to next level for another decomposition. The process is likewise for second and third level, etc. The following depicts the decomposition for *N* level.

For (n = 1 to N)

For (k = 0 to $K/2^n - 1$)

$$\begin{aligned}&\{c_n^H[k] = c_{n-1}^L[2k+1] - P\left\langle c_{n-1}^L[2k]\right\rangle;\\ &\ c_n^L[k] = c_{n-1}^L[2k] + U\left\langle c_n^H[k]\right\rangle;\ \}\\ &\text{end}\\ &\text{end}\end{aligned} \tag{8}$$

The operation unit $P(z)$ and $U(z)$ can be written as

$$P(z) = p\,(1 + z) \tag{9}$$

$$U(z) = q(z^{-1} + 1) \tag{10}$$

where p and q denote wavelet coefficient. Thus, under first-level decomposition, (8) is written as

$$c_n^H[k] = c_{n-1}^H[2k + 1] + p\{c_{n-1}^L[2k+2] + c_{n-1}^L[2k]\} \tag{11}$$

$$c_n^L[k] = c_{n-1}^L[2k] + q\{c_n^H[k] + c_n^H[k + 1]\} \tag{12}$$

Equation (11) and (12) show that we can utilize n same filter structure to implement N-level discrete wavelet transform. Figure 1 depicts the block diagram of proposed signal acquisition system using modified DWT.

NCO depicts the numerical controller oscillator. The function of the decision logic is that it separates signal from noise by thresholding wavelets coefficients. After carrier is removed, the signal $y_0[2k + 1]$ employing MDWT with first and second level is decomposed into different sub-bands, each of which has a different resolution and is termed "Analysis Filter Bank". In other word, we transform the input data $y_0[2k + 1]$ and the local replica *C/A* code to the wavelet domain to decrease, the length of signals used to calculate the product, of circular convolution by FFT. This is depicted as follows:

$$\begin{aligned}C_m(\tau, f_D) &= \sum_{k=1}^{M} \Lambda(s_2^L[k/2]) \cdot o_2^L[k/2+m]_M\\ &= \Lambda(s_2^L[k/2]) \otimes o_2^L[-k/2]\\ &= F^{-1}\left\{F\{\Lambda(s_2^L[k/2])\}F^*\{o_2^L[k/2]\}\right\}\end{aligned} \tag{13}$$

where "⊗" is convolution operator. F, F^{-1} and '*' denote FFT, inverse FFT and the complex conjugate operator, respectively. $\Lambda(\bullet)$ depicts the threshold function. Donoho's soft thresholding function is utilized [10], which is shown as follows:

$$\Lambda(x) = \begin{cases} x - \gamma\,\mathrm{sgn}(x) & |x| > \gamma \\ 0 & |x| \le \gamma \end{cases} \tag{14}$$

All coefficients are shrunk towards zero. A threshold parameter γ is related to the variance of the Gaussian noise. In particular, the MDWT method is iterated only on the lower band in order to achieve finer frequency resolution at lower frequencies. As a result, the lower band signals $s_2^L[k/2]$ are correlated with the low-pass filtered version of replica code $o_2^L[k/2+m]$, which also employs the DWT by circularly shifting the local replica and the m of which stands for the number of samples the replicated C/A code is phase shifted.

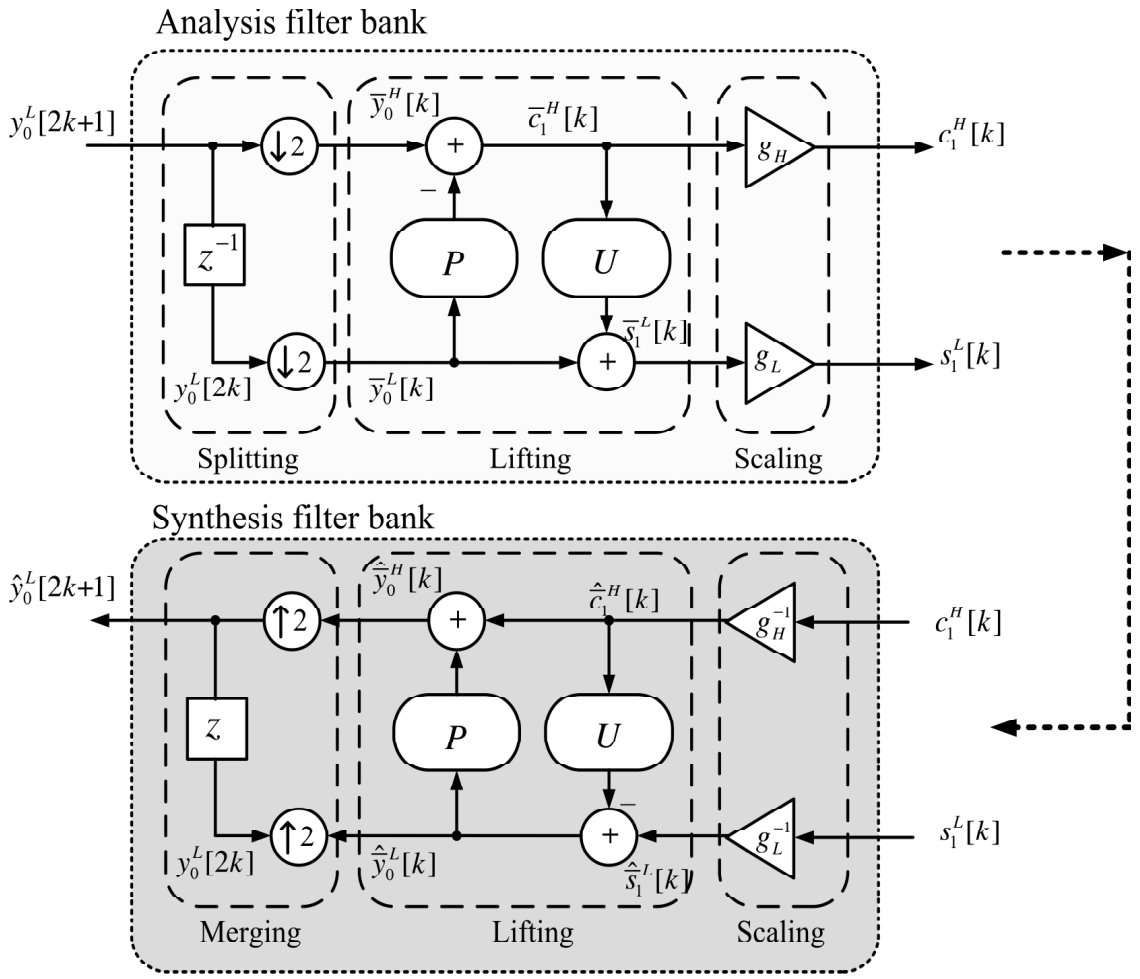

Figure 1: Block Diagram of Lifting Wavelet Transform and Inverse Transform

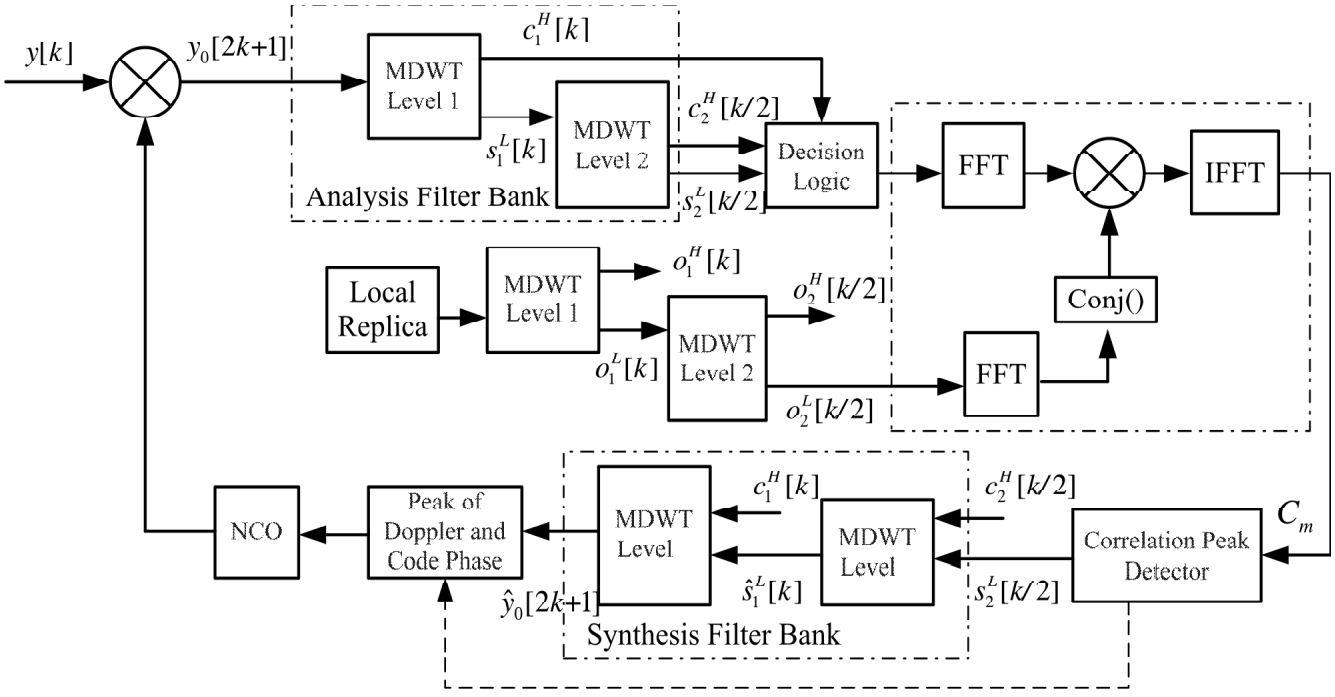

Figure 2: Wavelet-based Acquisition System

Equation (13) reveals that if the decision variable C_m exceeds the detection threshold determined by the noise statistics, the decision logic selects the corresponding C_m and the corresponding time delay as the estimated code phase. Finally, the output version C_m is reconstructed from the shrunk wavelet coefficients. That the halfband filters form the orthonormal bases makes the reconstruction in this case very easy. The above procedure is followed in reverse order for the reconstruction. The signals at every level are up-sampled by two, passed through the synthesis filters bank, and then added.

The major difference between MDWT and traditional FFT-based signal search method is that the MDWT-based signal search method can get rid of the redundancy of adopting traditional FFT-based search and only half or 1/4 samples are employed compared with traditional FF-based search. The same method can be executed by adopting signal decimation and interpolation, the results of which are less effective than those using MDWT as shown in experiment results section.

The reconstruction signal $\hat{y}_0[2k+1]$ is obtained through two level MDWT and circular convolution. Next, the corresponding code phase and Doppler shift in terms of $\hat{y}_0[2k+1]$ are sent to numerical control oscillator (NCO) to adjust code shift again. Once the code shift range is below 1/2 chip range, the code shift is sent to tracking loop for code tracking.

III. PERFORMANCE EVALUATION

During the internal signal processing of GPS receiver, signal acquisition loss often occurs at the front-end filter, A/D quantization error, the residual error of Doppler and code.

Under ideal conditions, assume the frontend does not essentially impact the signal component, the noise term entering the acquisition stage is a white sequence, the quantization impact is essentially negligible. This study simply considers the signal correlation loss caused by signal acquisition method. In this section, the influence of residual Doppler frequency and delay alignment error are presented. Meanwhile, the signal detection performance and acquisition system complexity are also analyzed.

(A) Correlation Loss

In the presence of Doppler and code misalignment, it is possible to demonstrate that the de-modulated component is shown as follows [11]:

$$\hat{Y}(\tau, f_D) = \sqrt{2\hat{P}}\,\mathrm{sin}\,c(K\delta_f)R(\delta_\tau)\exp(j\phi_0) + \eta_w \tag{15}$$

where $\hat{P}$ is the estimated signal amplitude, η_w is the noise term, $\delta_f = (f_C - f_D)/T_s$ is the normalized Doppler frequency error, δ_τ is the code phase residual error and $R(\bullet)$ is the normalized cross-correlation function between the local replica and the incoming GNSS signal. sin $c(\bullet)$ denotes the sinc function. Equation (1) shows that the frequency error δ_f is multiplied by the factor K that denotes the number of samples used to coherently integrate the input signal. The frequency error and code phase residual error is limited by the Doppler bin step size and size of the code phase search step, respectively, shown in the following:

$$|\delta_\tau| \le \frac{\Delta\tau}{2} \tag{16}$$

$$|\delta_f| \le \frac{\Delta f}{2} \tag{17}$$

The quality of the GNSS signal is usually measured at this stage [12, 13] by the so called *coherent output SNR* (*c-SNR*), defined as

$$c\text{-}SNR = \max_{\phi_0} \frac{\mathrm{E}^2\{\hat{Y}(\tau, f_D)\}}{\mathrm{Var}\{\hat{Y}(\tau, f_D)\}} \tag{18}$$

The coherent output SNR, under the effect of δ_f and δ_τ, (18) can be given by

$$\begin{aligned} c\text{-}SNR &= 2\hat{P}\sin c(K\delta_f)R^2(\delta_\tau)\frac{2K}{\sigma_w^2}\cos^2(\phi_0) \\ &= 2\frac{\hat{P}}{N_0}KT_s\sin c(K\delta_f)R^2(\delta_\tau)\cos^2(\phi_0) \end{aligned} \tag{19}$$

In (19), it is possible to define a loss associated with the Doppler frequency and code phase errors, which is called correlation loss function L_S, and is given by

$$L_S(\delta_f, \delta_\tau) = \sin c(K\delta_f)\, R^2(\delta_\tau) \tag{20}$$

To avoid the δ_f severely deteriorate signal acquisition performance, Δ_f is typically set below $2/3T_c$. The proposed method will employ (19) and (20) to analyze the generated correlation loss.

(B) Signal Detection Performance

With regards to signal detection method, decision making or hypothesis testing are often adopted to evaluate signal detection performance. To effectively analyze the signal detection performance of proposed, this study employs the signal detection theory proposed by Kay to assess GNSS signal detection performance. Two hypothesis tests and a pre-determined threshold are often utilized to determine whether signal exists in received set of observations. Such a problem is termed a binary hypothesis test (H_0 and H_1). The detector is susceptible to two error types due to noise interference. It is better to reduce both error probabilities as much as possible. However, a decrease in one probability is obtained at the expense of an increase in the other. Thus, an optimal detector can only minimize one error probability while constraining the other at a predetermined and acceptable level. In particular the detection P_D and the false alarm probabilities P_{FA} are defined as

$$\mathrm{P_D}(\alpha) = \rho(\bar{Y} > \alpha \,|\, \boldsymbol{H}_1) \tag{21}$$

$$\mathrm{P_{FA}}(\alpha) = \rho(\bar{Y} > \alpha \,|\, \boldsymbol{H}_0) \tag{22}$$

where α depicts decision threshold. The probability density function (PDF) under each hypothesis is given by $\rho(\bar{Y} > \alpha \,|\, \boldsymbol{H}_0)$ and $\rho(\bar{Y} > \alpha \,|\, \boldsymbol{H}_1)$. The plot of the detection probability versus the false alarm probability is called the Receiver Operating Characteristic (ROC). Although the ROC totally characterizes the detector performance [14], it is often helpful to have a single metric, the output or equivalent coherent SNR, which encapsulates as much information about the detector performance as possible. Thus, (8) and (9) are given by

$$\begin{aligned} c\text{-}SNR &= \max_{\phi_0, \delta_f, \delta_\tau} \frac{2\hat{P}}{N_0}KT_s\sin c(K\delta_f)R^2(\delta_\tau)\cos^2(\phi_0) \\ &= \frac{2\hat{P}KT_s}{N_0} = \frac{2\hat{P}T_c}{N_0} = \frac{\beta}{\sigma_w^2} \end{aligned} \tag{23}$$

In this way the ROC can be parameterized with respect to $\bar{\alpha} = \alpha/\sigma_w^2$, leading to the following expression:

$$P_D(\bar{\alpha}) = Q_1(\sqrt{c\text{-}SNR}, \sqrt{\bar{\alpha}}) \tag{24}$$

$$P_{FA}(\bar{\alpha}) = \exp\{-\bar{\alpha}/2\} \tag{25}$$

where $Q_b(*, o)$ is the generalized Marcum Q-function with *b*-order. The coherent output SNR denotes a fundamental metric for characterizing the acquisition performance. That is, the degradations owing to Doppler frequency and code phase errors can be directly expressed in terms of losses affecting $c\text{-}SNR$. These degradations have been elaborated in previous session.

(C) Computational Complexity

One significant feature of DWT is its considerably low complexity. Suppose the convolution is achieved through the FFT-based method, the complexity is of order $O(N \log_2 N)$. The computing time is longer than the one achieved through the wavelet transform, where the complexity is in proportion to $O(N)$. The symbol N stands for the signal length. Even in (4), circular convolution operator is adopted. The length obtained with this method is half the length acquired by FFT-based method, resulting in shorter signal acquisition time. Table 1 illustrates the hardware implementation complexity and performance evaluation of different methods. The analysis is conducted in terms of operation time, acquisition margin, precision of parameters and complexity. Assume the data length of 1ms is 5000 samples and the original bandwidth and search range, search times fo Doppler frequency for each acquisition method are the same. The result of signal acquisition sensitivity is obtained through 300 Monte Carlo simulations. The execution time is measured using the tic and toc functions in MATLAB software. An average PC (Pentium Dual-Core 1.6 GHz) is used for execution time measurements, which are made 30 times, and the mean of which is computed. However, the relative measures should point out which method has the greatest potential to be implemented in real-time application. During signal search stage, the optimal range of code estimation error is 0.5 chip space. Table 1 shows that the use of decimation FFT-based method for signal acquisition takes shorter computation time, which results from reduced number of samples. Meanwhile, this method doesn't require additional filter process. However, this method is inferior to other methods in the precision of signal parameter and interference tolerance. The use of discrete wavelet transform is not only robust in signal acquisition performance but also its acquisition time is within tolerable range. However, this method is limited in that the filter structure is high in complexity and not easy to implement. The proposed lifting-circular based discrete wavelet transform method can be implemented in terms of integer addition and shift operatio, which results in shorter computation time. Besides, this method can yield better signal and sensitivity. With regards to hardware implementation complexity, as a case study, in a traditional form, the computations of K-point FFT/IFFT algorithm takes K (K/2) $\log_2$ complex multiplications and $K \log_2 K$ complex additions. With regards to the suggested method, the computations of K-point FFT algorithm takes (K/2) $\log_2 K$ complex multiplications and $K \log_2 K$ complex additions, whereas that of K/Q point IFFT requires (K/2κ) $\log_2$ (K/κ) complex multiplications and (K/κ) $\log_2$ (K/κ) complex additions. κ denotes the reduction factor based on assistance data. Assume the search is to be conducted in frequency, an additional parameter f_b which is the number of frequency bins to be searched is taken into account. Wavelet transform method does not require much additional hardware resource. With respect to the second-level filter designed in lifting-convolution based WDT, it only additionally takes 6 multipliers and eight additions.

The total number of computations required to perform the whole convolution when the FFT of the replica is done externally, in different modes is illustrated in Table 1. it is obvious that the proposed GPS system acquisition is less complex than both FFT search algorithm and signal decimation approach since it takes a small number of operations to execute out the convolution operation.

Table 1
Performance Comparison of Different Acquisition Method

		Decimation FFT-based Method [15, p. 459].	*Time/frequency-domain search*	*DWT method [7] [8]*		*MDWT method*	
				(One-level decomposition)	*(Two-level decomposition)*	*(One-level decomposition)*	*(Two-level decomposition)*
Operation time (sec)		1.63 ($\kappa = 2$)	5.45	2.23	1.22	2.03	1.13
Precision	Doppler frequency resolution	120 Hz	55 Hz	75 Hz	95 Hz	70 Hz	85 Hz
	Code phase error	0.9 chip	0.22 chip	0.39 chip	0.48 chip	0.38 chip	0.42 chip
	Level	Low	High	Medium-High	Medium	Medium-High	Medium
Sensitive (SNR in dB)		-14.24 dB	-15.01 dB	-16.14 dB	-16.84 dB	-16.04 dB	-16.90 dB
Complexity	Multipliers	$(K/2)\log_2 +$ $f_b \cdot (K + (K/2\kappa)\log_2(K/\kappa))$	$(K/2)\log_2 K +$ $f_b \cdot (2K + (K/2)\log_2 K)$	$4+(K/2)\log_2 +$ $f_b \cdot (K + (K/4)\log_2(K/2))$	$6 + (K/2)\log_2 +$ $f_b \cdot (K + (K/8)\log_2(K/4))$	$2 + (K/2)\log_2 +$ $f_b \cdot (K + (K/4)\log_2(K/2))$	$6 + (K/2)\log_2 +$ $f_b \cdot (K + (K/8)\log_2(K/4))$
	Adders	$K\log_2 K +$ $f_b \cdot (K + (K/\kappa)\log_2(K/\kappa))$	$K\log_2 K +$ $f_b \cdot (K\log_2 K)$	$9 + K\log_2 K +$ $f_b \cdot (K + (K/2)\log_2(K/2))$	$14 + K\log_2 K +$ $f_b \cdot (K + (K/4)\log_2(K/4))$	$4 + K\log_2 K +$ $f_b \cdot (K + (K/2)\log_2(K/2))$	$8 + K\log_2 K +$ $f_b \cdot (K + (K/4)\log_2(K/4))$
	Level	Low	High	Medium	Medium	Medium- Low	Low

IV. SIMULATION RESULTS

In this section, simulation results are depicted to evaluate the performance of the proposed method. The frequency search range is ±5 KHz, and the FFT length is assumed as one msec (5000 samples), which is the same as the period of C/A code. The tests are performed and each result is obtained through 250 independent Monte Carlo simulations. To verify the performance of the proposed method, it is compared with traditional FFT-based method [3] and reduced length of FFT method (decimation). The reason for employing decimation of the GPS signal is to reduce the size of the data set and optimize the data set size for the FFT-based algorithm.

(A) Signal Detection Probability

The acquisition performance can be obtained analytically integrating (21) and (24). Both the detection and false alarm probabilities are acquired based on Monte Carlo computer simulations. That is, the probabilities are obtained dividing the number of successful events by the overall number of trials. This comparison is presented in Fig. 3 for the ROC curve in the case of a P/N_0 = 32 dB-Hz.

Figure 4 shows that the detection probabilities for the different acquisition techniques have been plotted for different values of P/N_0 and for a fixed false alarm rate $P_{FA} = 10^{-2}$. It is obvious from the plot that MDWT method outperforms the other acquisition strategies, since, for a given P/N_0, it yields the highest detection probability. In this case, since the probability of false alarm is lower than 0.1, decimation FFT method outperforms the time/frequency FFT strategy.

(B) Signal Detection Probability in Presence of Losses

Figure 5 reports the Receiver Operating Characteristic (ROC) which depicts the probability of detection versus the probability of false alarm. The curve has been obtained considering the integration of a single

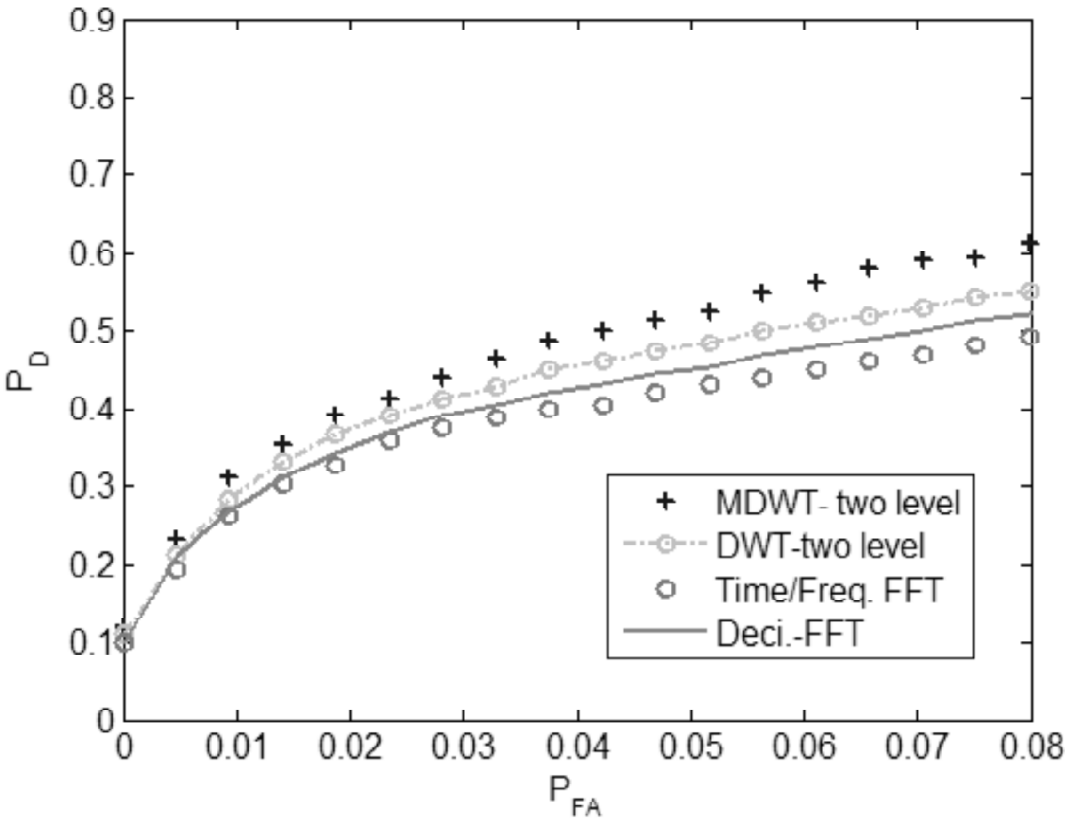

Figure 3: ROC Curve Calculated for a P/N_0 = 32 dB-Hz

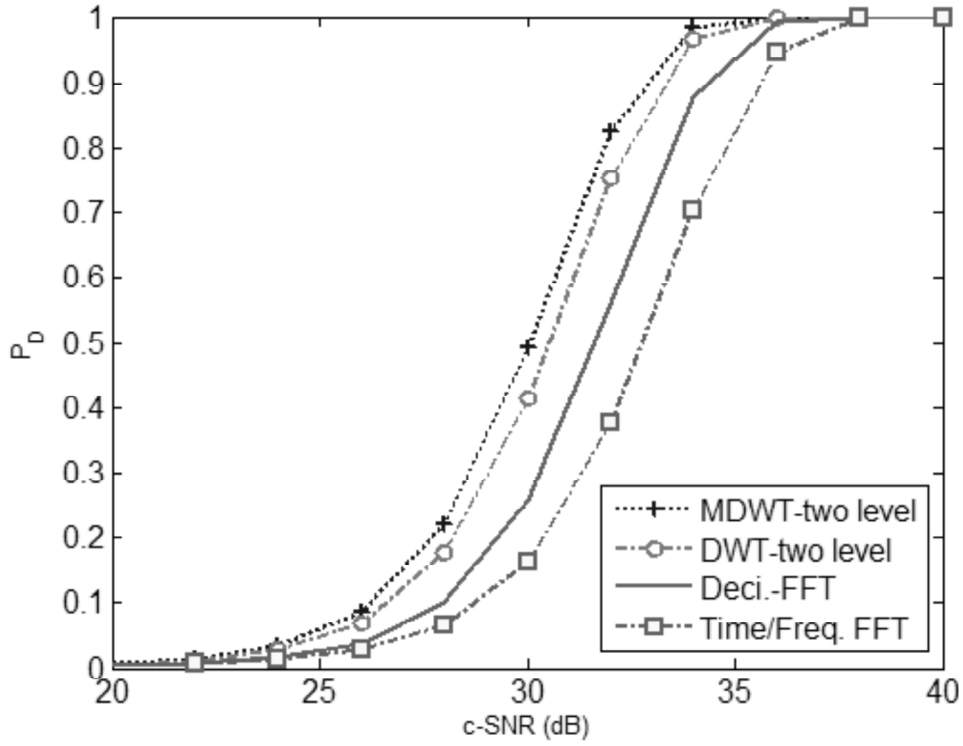

Figure 4: *c-SNR* Comparison for the Simulated Results for the GPS PRN Signal and Desired $P_{FA} = 10^{-2}$

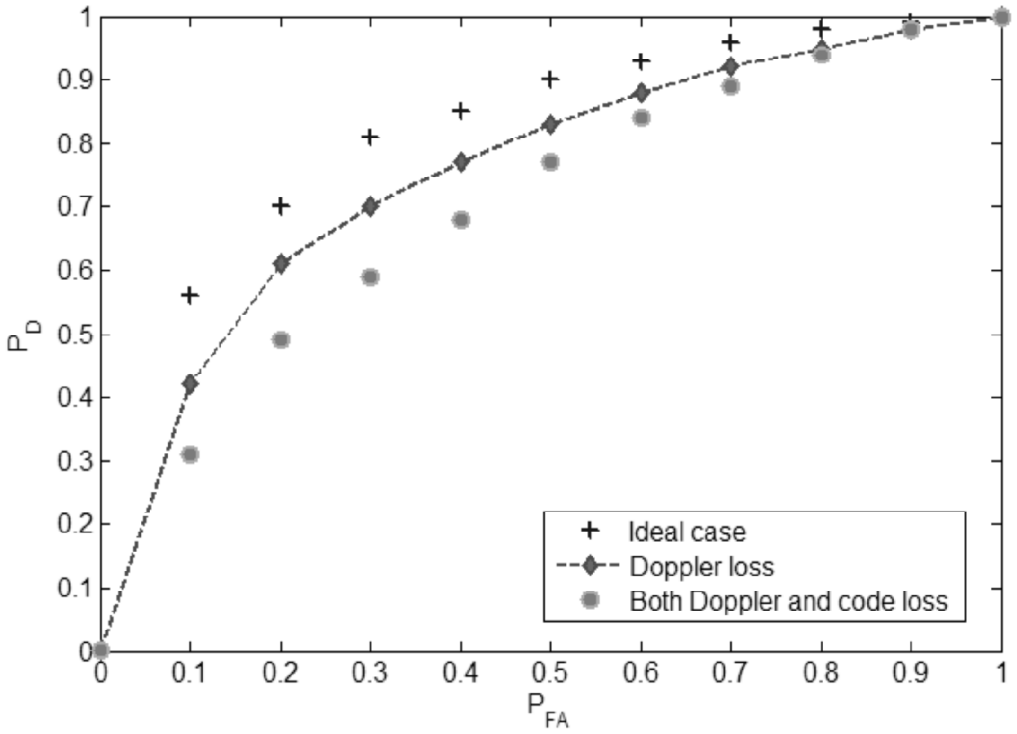

Figure 5: Loss Contribution Comparison, ROC Curve for the GPS PRN Signal and P/N_0 = 32 dB-Hz

GPS PRN code period, an IF filter bandwidth of 2MHz, a carrier to noise ratio P/N_0 = 32 dB-Hz, and a sampling frequency of about 5 MHz, which leads to a code ambiguity resolution of half a PRN slot. Figure 6 is the graph that shows the detection probability versus the P/N_0 ratio for a false alarm probability $P_{FA} = 10^{-2}$, for a GPS PRN signal, and with the same receiver parameters of Fig. 5. It is here important to

remark how considerable is the loss of acquisition performance due to the Doppler and code misalignment with respect to the ideal case. Moreover it has to be considered that the curves which report the performance when both the code and Doppler loss are considered have been obtained in an average misalignment condition (both code and Doppler error uniformly distributed in the cell area), and so, they do not represent the worst case.

V. EXPERIMENT RESULTS

This section demonstrate the experiment results to verify the feasibility of the proposed method to shorten the acquisition time. The digital samples are obtained through a PCI-based data acquisition board through data acquisition software. The data samples from antenna element are stored and, then, post-processed for signal acquisition analysis. The frequency search range is ±10 KHz, and the FFT length is assumed as one msec (16368 samples), which is the same as the period of C/A code. The false alarm rate is choosen to be 0.01, and the signal detection probability is then computed. Detection threshold is 22 dB with a lowest value of carrier to noise ratio (CNR) 35 dB-Hz for one msec noncoherent integration time. The Haar functions are the basis of mother wavelet.

The test was conducted in Tainan city, Taiwan. Eight GPS satellites are observed. The signal (PRN17) is located at azimuth 295° and elevation 30°. In the experiment, 30 ms data sets are stored to verify the feasibility of the proposed method. In each experiment, the receiver is turned on to receive GPS signals and the nominal acquisition margin ratio with respect to each satellite is computed. The margin ratio is determined as maximum peak of correlation value to mean of rest peak ratio.

Figure 7 illustrates the results of acquisition from different search methods for PRN17. It is observed that all search methods find the coarse Doppler frequency and code delay of the signal. Table 2 compares the performance of proposed method with those of the Time/frequency-domain search method. The execution time is measured using the “tic” and “toc” functions in MATLAB software. An average PC (Pentium Dual-Core 1.6 GHz) is used for execution time measurements, which are made 30 times, and the mean of which is computed. However, the relative measures should point out which method has the greatest potential to be implemented in real-time application. The acquisition margin for PRN17 using the different search methods is also shown in Table 2. It is shown that the proposed method has higher acquisition margin than the others.

Table 2
Performance Comparison of three Search Methods with Regard to PRN17

Method	*Execution time (sec)*	*Acquisition Margin (dB)*	*Complexity (Multiplier plus additions)*
Time/frequency-domain search (16368 samples)	3.246	18.1059	High
Decimation FFT-based Method (8184 samples)	2.471	11.7623	Medium
DWT method (one-level decomposition; 8184 samples)	1.494	21.4387	Medium
DWT method (Two-level decomposition; 4092 samples)	1.673	17.764	Low

VI. CONCLUSION

In this study, a lifting-circular wavelet scheme is proposed successfully to acquire GNSS signals. The efficiency of proposed scheme counts on the number of terms in the wavelet transform. It helps to perform a FFT on 1250 points without deteriorating the performance of the acquisition system. The wavelet transform application can concentrate the energy of the signal in some coefficients, which renders it possible to apply a FFT to a reduced number of points. Thus, it can simplify the complexity of the acquisition system and facilitate this implementation.

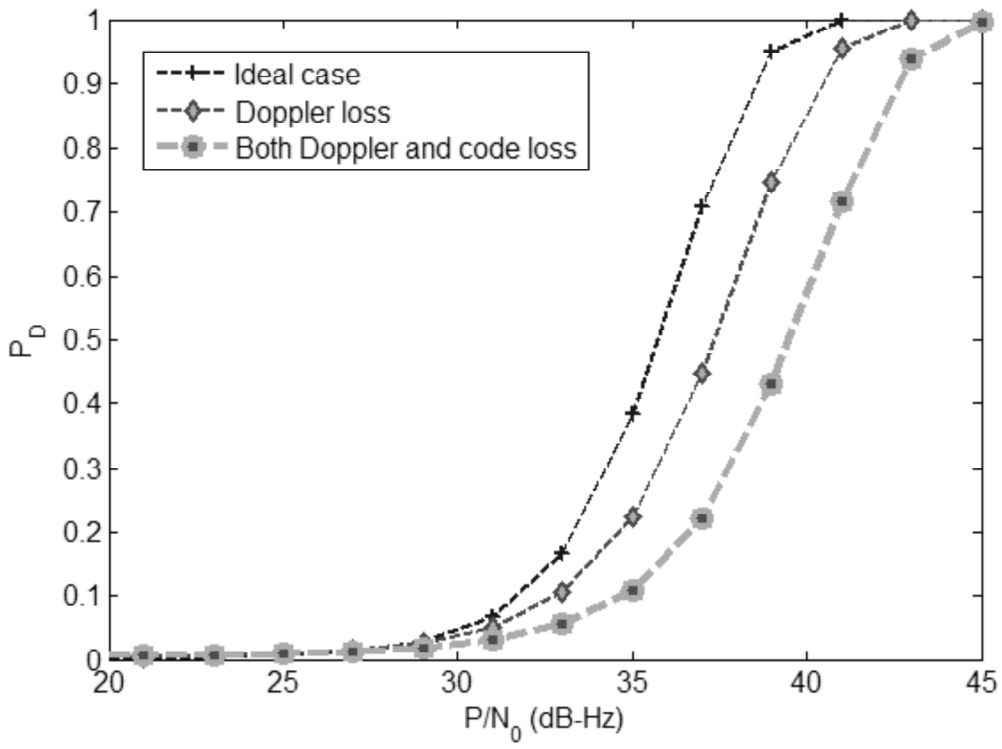

Figure 6: Loss Contribution Comparison, Curve for the GPS PRN Signal and Desired $P_{FA} = 10^{-2}$.

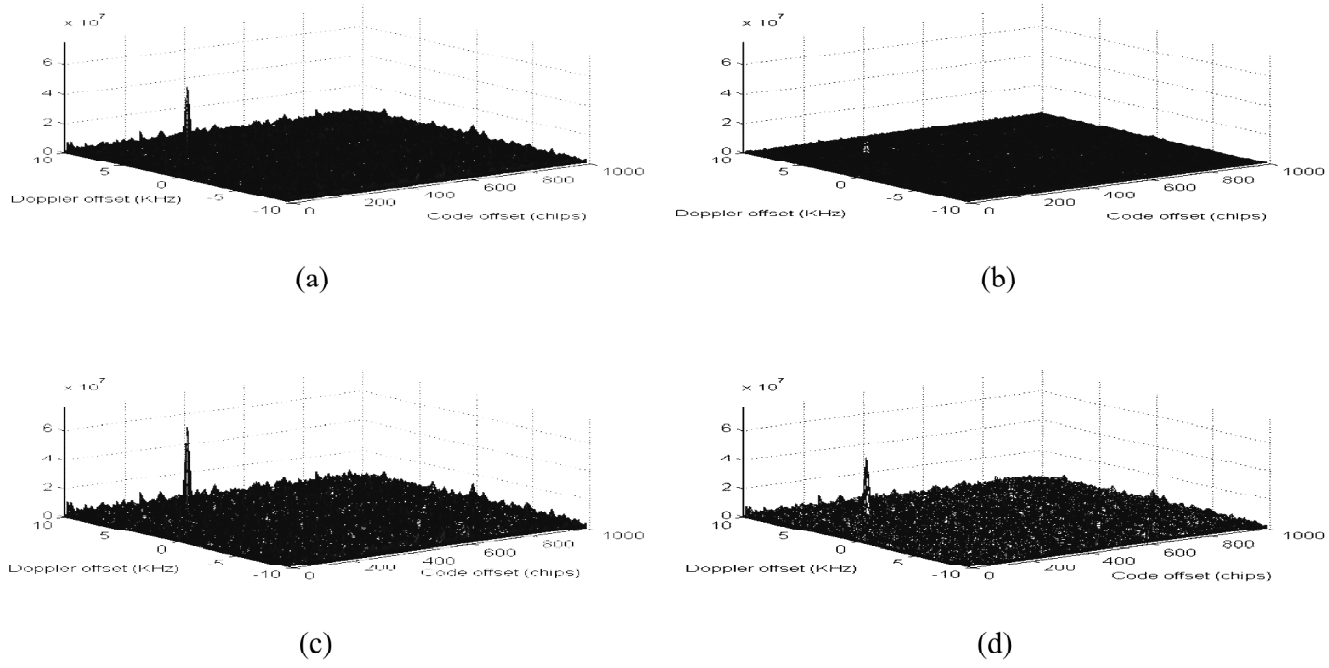

Figure 7: Acquisition Results from Different Signal Search Method for PRN17; (a) Time/Frequency-domain Search Method (16368 Samples) (b) Decimation FFT-based Search Method (from 16368 to 8184 Samples) (c) One-level DWT Method (from 16368 to 8184 Samples) (d) Two-level DWT Method (from 16368 to 4092 Samples)

Meanwhile, different realizations of the FFT-based search methods are also assessed. The simulation results demonstrate that the proposed scheme can save signal search time and its low complexity can satisfy real-time processing in contrast to traditional FFT-based and decimation-based methods.

ACKNOWLEDGEMENTS

The authors would like to thank the National Science Council of Taiwan for their support of this work under grant 102-2221-E-020-007.

REFERENCES

[1] M. Braasch, A. Van Dierendonck, "GPS Receiver Architectures and Measurements," *Proc. IEEE*. **87**(1): 48–64, 1999.

[2] M. L. Psiaki, "Block Acquisition of Weak GPS Signals in a Software Receiver," in *14th International Technical Meeting of the Satellite Division of the Inst. of Navigation* (*ION GPS*), pp. 2838–2850, Salt Lake City, Sep. 2001.

[3] D. Akopian, "Fast FFT Based GPS Satellite Acquisition Methods," *IEE Proc. Radar Sonar & Navig.*, **152**(4): 277–286, 2005.

[4] P. K. Sagiraju, G. V. S. Raju, and D. Akopian, "Fast Acquisition Implementation for High Sensitivity Global Positioning Systems Receivers Based on Joint and Reduced Space Search," *IET Radar Sonar & Navig.*, **2**(5): 376–387, 2008.

[5] I. Daubechies, "Orthonormal bases of Compactly Support Wavelets," *Comm. Pure Appl. Math.*, **41**: 909-996, 1988.

[6] S. G. Mallat, "A Theory for Multiresolution Signal Decomposition: The Wavelet Representation," *IEEE Trans. on Pattern Analysis and Machine Intelligence*, **11**(7): 674–693, 1989.

[7] J. T. Liu, "A Novel GNSS Weak Signal Acquisiton Using Wavelet Denosing Method," ION ITM, 2008.

[8] C. L. Chang, H. N., Shou, and J. C. Juang, "Wavelet-based Method for Signal Acquisition in GNSS Receivers," *SICE Annual Meeting*, pp. 1261–1264, Taipei, Taiwan, Aug. 2010.

[9] W. Sweldens, "The Lifting Scheme: A Custom-design Construction of Biorthogonal Wavelet," *Applied and Computational Harmonic Analysis*, **3**(2): 186–200, 1996.

[10] D. L. Donoho, "De-noising by Soft-thresholding," *IEEE Trans. Info. Theory*, **41**: 613–627, 1995.

[11] B. W. Parkinson and J. J. Spilker, Eds., *Global Positioning System: Theory and Applications*. American Institute of Aeronautics and Ast (AIAA), **1**, 1996.

[12] J. W. Betz, "Effect of Narrowband Interference on GPS Code Tracking Accuracy," in *Proc. of ION National Technical Meeting*, pp. 16–27, Anaheim, CA, Jan. 2000.

[13] J. W. Betz, "Effect of Partial-band Interference on Receiver Estimation of *C/N*0: Theory," in *Proc. of ION National Technical Meeting*, pp. 817–828, Long Beach, CA, Jan. 2001.

[14] J. V. DiFranco, and W. L. Rubin, *Radar Detection*. Dedham, Artech House Inc., MA, 1980.

[15] J. G. Proakis and D. G. Manolakis, *Digital Signal Processing: Principles, Algorithms, and Applications*. Prentice-Hall, Englewood Cliffs, NJ, 1996.